Thin film confinement effects on the thermal properties of model photoresist polymers

Christopher L. Soles,[a] Eric K. Lin, Joseph L. Lenhart, Ronald L. Jones, and Wen-li Wu
NIST Polymers Division, Gaithersburg, Maryland 20899-8541

Darío L. Goldfarb and Marie Angelopoulos
IBM T. J. Watson Research Center, Yorktown Heights, New York 10598

(Received 1 June 2001; accepted 10 September 2001)

The demand to print increasingly smaller microelectronic device features means that the thickness of the polymer films used in the lithographic processes must decrease. The thickness of these films is rapidly approaching the unperturbed dimensions of the polymer, length scales at which confinement deviations and dewetting are a significant concern. We combine specular x-ray reflectivity (SXR) and incoherent neutron scattering (INS) to probe the thermal stability and dynamical effects of thin film confinement in poly(hydroxy styrene) (PHS), a polymer used in a majority of the 248 nm deep UV photoresists. PHS forms stable thin films (down to 5 nm) that do not dewet over a wide temperature range on Si surfaces ranging from hydrophilic to hydrophobic. The surface energy has a profound influence on the magnitude of the thin film expansion coefficient, especially above the glass transition, in films as thick as 100 nm. Confinement also appears to suppress the mean-square atomic displacements and the level of anharmonicity in the dynamics, primarily above the bulk glass transition. © *2001 American Vacuum Society.*
[DOI: 10.1116/1.1415502]

I. INTRODUCTION

As the semiconductor industry continues to improve upon chip functionality and speed, there are increasingly stringent lithographic demands to print smaller and more uniform device features. While state-of-the-art deep UV lithographic processes print 180 nm features using 248 nm radiation, smaller features necessitate shifts to shorter wavelengths. Unfortunately, most polymers are highly absorbing at the anticipated 193 and 157 nm wavelengths and the extremely deep UV radiation is not able to completely penetrate the lithographic film. This can be overcome by utilizing bilayer resists where only a thin top layer is photoactive. To ensure UV transparency, the thickness of this photoactive layer should be 100 nm or less.

A sub-100 nm layer introduces a new class of problems related to the integrity or stability of the resist film. These length scales approach the unperturbed dimensions of the macromolecule and confinement induced property deviations need to be considered. For example, it is documented that a polymer glass transition temperature (T_g) can decrease,[1–9] increase,[8–13] or remain constant[14,15] when the film thickness approaches a few multiples of the radius of gyration (R_g), with shifts as great as $\pm 50\,^{\circ}\mathrm{C}$ reported. Thin film confinement can also induce spinodal dewetting[16,17] in some instances. Clearly these issues are of extreme relevance to the lithography community. The postapply and postexposure bakes in image development are typically within $20-30\,^{\circ}\mathrm{C}$ of the bulk polymer T_g. In addition to the danger of dewetting, T_g depressions could lead to diffusion between the exposed and unexposed regions of a pattern, resulting in image blur. It is of paramount importance for the future resist technologies to understand the effects of confinement on lithographic films.

In this article we address thin film confinement issues in poly(hydroxy stryrene) (PHS), a ''workhorse'' lithographic polymer for use with 248 nm radiation, using both specular x-ray reflectivity (SXR) and incoherent neutron scattering (INS). SXR measures the uniformity and thickness of PHS films supported on various substrates as a function of temperature. The T_g is typically inferred from a kink in the thin film thermal expansion curve. On the other hand INS directly probes the dynamics of a hydrogenous polymer by measuring the amplitude of the average mean-square atomic displacements $\langle u^2 \rangle$. It is well documented that $\langle u^2 \rangle$ in bulk glasses shows a sudden increase near T_g.[18–20] Together these techniques start to provide a general understanding of how thin film confinement affects the dynamics of PHS.

II. EXPERIMENT

Two grades of PHS, with number average relative molecular masses of 2.5 and 8 kg/mol, were dissolved in propylene glycol methyl ether acetate (PGMEA) at mass fractions of 0.2%, 0.5%, 1.0%, and 5.0%. These solutions were filtered through a 0.2 μm Teflon filter and spun coat onto silicon wafers with three different surface treatments. The surface energies ranged from hydrophilic (native oxide of silicon, SiO_x), intermediate (silicon nitride, SiN_x), to hydrophobic (hydrogen passivated silicon, SiH). The SXR experiments were performed on a modified Scintag (Santa Clara, CA)[21] diffractometer under a vacuum of $10^{-4}-10^{-5}$ Pa. While the SiO_x and SiN_x substrates are stable under atmospheric conditions, the SiH is relatively unstable and reverts to an oxide within hours after passivation with ammonium fluoride. To prevent oxide regrowth, the PHS films were spun

[a]Author to whom correspondence should be addressed; electronic mail: csoles@nist.gov

coat onto SiH substrates immediately after passivating and quickly transferred to the high vacuum chamber of the reflectometer. Prior to all reflectivity experiments, the PHS films were annealed for 12 h at 200 °C (under a 10^{-4}–10^{-5} Pa vacuum) to remove residual solvent. Subsequent expansion curves were obtained by collecting reflectivity curves as a function of temperature between 200 and 20 °C in increments of 10 °C. After each temperature change, 45 min was allocated for thermal equilibration with 1 h required to collect the reflectivity data. The results from multiple heating and cooling runs, with 6 h equilibration allowed between each heating and cooling cycle, were then fit with nonlinear least-squares recursive multilayer algorithm[22] to extract the film thickness.

The incoherent neutron scattering in most polymers is dominated by H, which has a scattering cross section approximately 20 times larger than either C or O, and nearly 40 times larger than a Si wafer. In other words, the hydrogenous moieties of polymer will dominate the incoherent scattering for a PHS film supported on a Si wafer. Films for the INS experiments were prepared under identical conditions to the reflectivity samples, with the exception that only the SiO_x substrates were investigated. To obtain sufficient scattering signal from the thin films, several (13–15) Si wafers (diameter=75 mm) were broken into rectangular strips and placed in the sample cell. The incoherent elastic neutron scattering intensity is proportional to the Debye–Waller factor such that:

$$I_{\mathrm{inc}}(Q) \propto e^{-1/3\,Q^2\langle u^2\rangle}, \tag{1}$$

where Q is the scattering vector and $\langle u^2\rangle$ is the mean-square displacement. In this framework, the slope of $\ln[I_{\mathrm{inc}}(Q)]$ vs Q^2 yields $\langle u^2\rangle$, which can be tracked as a function of temperature. The INS experiments were performed at the NIST Center for Neutron Research on the high flux backscattering spectrometer located on the NG2 beamline.[23] The spectrometer operates with a neutron wavelength of 6.271 Å over a Q range of 0.25–2.0 $Å^{-1}$. The fact that the first Bragg peak for Si occurs at $Q \approx 2.67$ $Å^{-1}$ ensures that the dynamics of the Si substrates have a negligible contribution to the scattering intensity. The energy resolution of the spectrometer is 0.8 μeV, which implies that motions slower than 200 MHz are ''static'' and not reflected in $\langle u^2\rangle$.

III. RESULTS AND DISCUSSION

Figure 1 displays a series of SXR curves obtained at 150 °C for the 2.5 kg/mol PHS films on the SiO_x substrates. The film thickness is inversely proportional ($D \approx 2\pi/\Delta Q$) to the periodicity of the interference fringes, with fits[22] indicated by the solid lines. Clearly there is excellent agreement between the fits and experimental data. In this work, a satisfactory fit is obtained if the PHS film is modeled as a single polymer layer of uniform density. Figure 1 demonstrates that by changing the mass fraction of PHS in PGMEA from 0.2% to 5.0% the film thickness can be varied from roughly 40 to 1100 Å. This is precisely the thickness range (sub-100 nm)

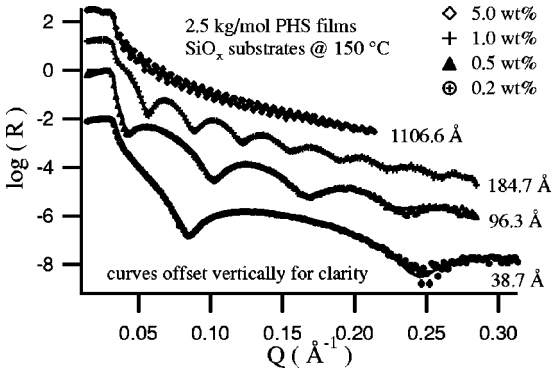

FIG. 1. Specular x-ray reflectivity curves for a series of PHS films supported on the SiO_x substrates. Fits to the experimental data are indicated with the solid lines. The standard uncertainty in the reflected intensity is less than the size of the symbols.

where deviations in the polymer properties are anticipated to be an issue in lithographic thin film imaging.

Figure 2 displays a series of thermal expansion curves for the 2.5 kg/mol PHS films supported on the SiO_x substrate. The expansion is presented in terms of a thermal strain, or percent change in thickness, arbitrarily relative to the film thickness at 180 °C. For the sake of clarity, the curves are offset vertically. The isothermal error bars are obtained from two heating and cooling cycles, resulting in four thickness determinations per temperature. At each temperature the spread in the data points is recorded with the average spread over all temperature reported as the isothermal error in thickness. In terms of a thermal strain, this average spread is on the order of $\pm 0.25\%$.

The general form of the expansion curves in Fig. 2 is typical for both PHS molecular weights and all substrates. A small molecular mass change from 2.5 to 8.0 kg/mol produces negligible differences in the expansion curves. The thicker films exhibit bulk-like expansion with a discontinuity near the bulk calorimetric T_g of 150 °C in PHS. However, as the film thickness drops below 100 nm (1000 Å), an interesting negative CTE is observed below the bulk glass transition temperature; the films appear to increase in thickness upon cooling. The magnitude of the negative CTE effect increases as the film thickness decreases, with the 40 Å film showing a negative CTE over almost the entire temperature

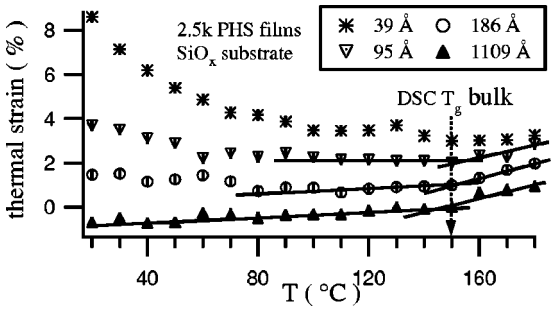

FIG. 2. Thin film thermal expansion curves (percent change in thickness) for the 2.5 kg/mol PHS films supported on the SiO_x substrates. The curves are offset vertically, and the standard uncertainties are described in the text.

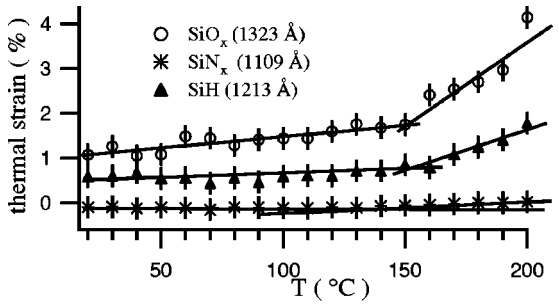

FIG. 3. Substrate effects on the thermal expansion in the thickest PHS films. Even in 1100–1300 Å films, the substrate surface energy has a profound influence on the coefficient of thermal expansion. However, significant shifts in the apparent glass transition temperature are not observed.

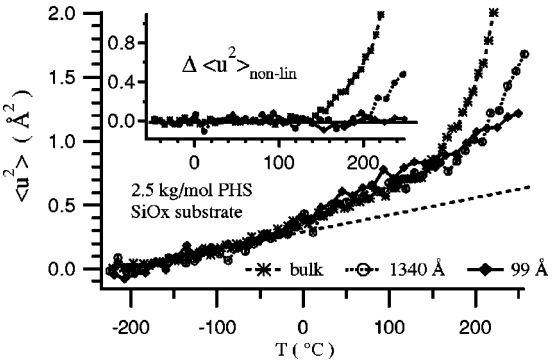

FIG. 4. $\langle u^2 \rangle$ as a function of T for 2.5 kg/mol PHS on the SiO$_x$ substrates. A low T onset of anharmonicity is observed deep in the glassy state (dashed line) and not affected by confinement. The evolution of $\langle u^2 \rangle$ beyond this point is approximately linear, with a very strong deviation from linearity near the bulk glass transition. These deviations from linearity (emphasized in the inset) are heavily dependent on confinement, with the inset axis having same units as the main graph.

range. A similar negative CTE is observed on all three substrates with both molecular weights. At this time, the origins of this negative CTE are not completely understood. We shall return to this issue later in the discussion.

Figure 3 compares the effect of substrate surface energy on the three thickest films (nominally 1100–1300 Å) with the curves offset vertically for clarity. Within experimental error, the data do not appear to support a significant shift of the apparent glass transition temperature when the substrate surface energy changes from hydrophilic to hydrophobic. However, it appears that the intermediate surface energy substrate (SiN_x) significantly reduces CTE in comparison to either SiO_x or SiH. This implies that the interactions between the substrate and the PHS are greatest for the SiN_x surface. This is somewhat surprising given the relatively high hydroxyl content of PHS. One might anticipate stronger interactions with the hydrophilic SiO_x surface, which also contains hydroxyls. It is also noteworthy that despite the lack of a noticeable shift in the apparent T_g, the magnitude of the thermal expansion coefficients shows a strong dependence on the surface energy of the confining substrate, even in films as thick as 100 nm. This thickness is well within the range of concern for the resist community and emphasizes that confinement deviations are not limited to shifts in the apparent T_g. A reduced expansion coefficient corresponds to a reduced molecular mobility, or a decrease in the level of anharmonicity. It remains to be seen if this reduced mobility has an impact on relevant lithographic processes, such as photoacid diffusion, dissolution, or reactive ion etching.

Figure 4 compares the thermal evolution of $\langle u^2 \rangle$ in relatively thick and thin PHS films (on SiO_x substrates) to the bulk material. The curves were obtained by slowly heating the samples (0.5 °C/min for the bulk and 1340 Å films, and 0.1 °C/min for the 99 Å films) between -225 and 250 °C. The elastic scattering intensities are binned into 5–10 °C intervals, and $\langle u^2 \rangle$ is calculated from the linear slope of $\ln[I_{inc}(Q)]$ vs Q^2 at each interval [see Eq. (1)]. We assume that at -225 °C nearly all the mobility is quenched from the system and thereby define $\langle u^2 \rangle = 0$ at this point. At low temperatures (below -75 °C), $\langle u^2 \rangle$ evolves linearly with T, characteristic of a harmonic solid. Between -75 and -50 °C there is a gentle, but clear, deviation from linearity indicating the onset of anharmonic motions. Such an anharmonicity of $\langle u^2 \rangle$ deep in the glassy state is documented in a broad range of glassy polymers and typically ascribed to side group rotations, C–C torsions, etc., in most polymers.[18,19] While the precise origin of the sub-T_g anharmonicity in PHS is yet to be identified, the coincidence of the bulk and confined $\langle u^2 \rangle$ in this regime indicates that these localized glassy motions are not affected by thin film confinement.

Figure 4 also reveals a sudden increase in the amplitude of $\langle u^2 \rangle$ of the bulk PHS near the DSC T_g. This indicates a sudden increase in the anharmonicity of the motion and a large increase in mobility. As the level of thin film confinement increases, this strong anharmonicity is suppressed and there is a decrease in $\langle u^2 \rangle$ above the calorimetric T_g. In the temperature range between the low T onset of local motions (approximately -75 °C) and the bulk T_g, the evolution of $\langle u^2 \rangle$ can be approximated as linear. The inset of Fig. 4 emphasizes the deviations from this linear dependence in terms of $\Delta \langle u^2 \rangle_{non\text{-}lin}$. Clearly, confinement suppresses the nonlinear or highly anharmonic motions associated with the glass transition. In the 1340 Å films the deviation from linearity shifts to higher T in comparison to the bulk, and is nearly absent in the 99 Å films.

These results might be interpreted as an increase, or even suppression, of the T_g of PHS upon thin film confinement. However, at this time we refrain from making this assertion. T_g's are conventionally defined by macroscopic volumetric or viscosity changes that occur on laboratory time scales of tens to hundreds of seconds. The motions reflected in $\langle u^2 \rangle$ are several orders of magnitude faster (pico- to nanosecond) and it remains to be seen how the two very different motions are related. An upward T shift for the deviation from linearity to 180 °C in the 1340 Å films is nominally consistent with thermal probe[10] and ellipsometry[9] T_g measurements on confined PHS films by Fryer and co-workers. In comparison to our SXR data in Fig. 2, the kink in the expansion curve for the 1109 Å film occurs closer to 150 °C, ~30 °C lower than the $\langle u^2 \rangle$ discontinuity. Although the experimental scatter be-

comes significantly greater, the expansion data in Fig. 2 for the 95 Å films *might* suggest a kink in the neighborhood of 150–160 °C, whereas similar deviations are not encountered in the $\langle u^2 \rangle$ data. However, SXR data are not of sufficient quality to make such a claim. The noise is considerable and also the SXR curves do not extend to high enough T (because of instrumental limitations) for a complete comparison of the two techniques. Furthermore, the negative CTE in the SXR data at lower T (especially in the thinner films) precludes an objective determination of an analogous deviation from linearity. For all of these reasons, we abstain from making claims regarding a precise T_g value using the two techniques.

It is intriguing that the negative CTE in Fig. 2 is not reflected in $\langle u^2 \rangle$. This raises several issues regarding the origin of this effect. The absolute magnitude of the increase in thickness upon cooling is small, on the order of a few angstroms for a 100 Å film. A similar negative CTE is also observed in thin polycarbonate (PC) films.[24] We established that the effect is not due to either a surface adsorption of small molecules from the vacuum chamber or the accumulation of water at the interface between the hydrophilic SiO_x surface and the polymer. In the PC films the effect was reproducible, but became noticeably pronounced with the onset of irreversible dewetting. We do not see signs of dewetting in the PHS films studied here. The fact that the effect is not evident in $\langle u^2 \rangle$ might be consistent with a surface induced molecular reorganization that affects one or two monolayers. This would be reflected in SXR, which is sensitive to the overall thickness, while $\langle u^2 \rangle$ represents a dynamical average throughout the film thickness.

The data presented here contain several features worth emphasizing for lithography. First and foremost is that PHS forms stable thin films, down to 50 Å in thickness, that do not display a strong tendency to dewet from a variety of surfaces, ranging from hydrophilic to hydrophobic. Dewetting would have been readily observed in SXR, but our multiple heating and cooling cycles produce reproducible expansion curves. However, we emphasize that the SXR expansion data are under vacuum and the reproducibility may suffer in air. This would probably result from thermal decomposition or crosslinking at temperatures near 200 °C. Test films of PHS on all three substrates were annealed at 200 °C for 12–24 h in both air and under vacuum (10^{-4}–10^{-5} Pa). The vacuum annealed films readily dissolved in acetone while air baked films were insoluble. This indicates that crosslinking/degradation can occur under atmospheric conditions at elevated temperature.

The second feature worth emphasizing is the decrease in the PHS mobility upon confinement above the bulk T_g, and the lack of change below. Buchenau[25] demonstrates an empirical exponential dependence of the viscosity η on $1/\langle u^2 \rangle$ in liquid and glassy Se. In this respect, a decrease in $\langle u^2 \rangle$ upon confinement points to a large increase in the viscosity of PHS above the glass transition. This is consistent with surface forces apparatus measurements on polymeric and small molecule liquid films revealing a dramatic increase in viscosity with greater confinement.[26] We suggest that $\langle u^2 \rangle$ is of the appropriate length and time scale (MHz) to affect transport of the H^+ ions requisite for the lithography photochemistry. This may be detrimental if image development takes place above T_g. However, the sub-T_g dynamics are not significantly affected by confinement, which suggests that acid transport below the glass transition may be similar in thick and thin lithographic films and is not a serious concern. This remains to be verified experimentally. It also remains to be seen if the different substrates lead to variations in $\langle u^2 \rangle$. As seen with the SXR expansion, changing the surface energy affects the CTE. As anharmonic motions are requisite for expansion, one might anticipate the suppression of $\langle u^2 \rangle$ to be greater on the SiN_x substrates.

ACKNOWLEDGMENTS

This work was funded in part by DARPA, Contract No. N66001-00-C-8803. C.L.S. and J.L.L. further acknowledge the NIST National Research Council Postdoctoral Program. The assistance from the NIST Center for Neutron Research and the valuable discussions with Rob M. Dimeo are also greatly appreciated.

[1] J. L. Keddie, R. A. L. Jones, and R. A. Cory, Europhys. Lett. **27**, 59 (1994).
[2] J. A. Forrest, K. Dalnoki-Veress, and J. R. Dutcher, Phys. Rev. E **56**, 5705 (1997).
[3] J. A. Forrest and J. Mattsson, Phys. Rev. E **61**, R54 (2000).
[4] K. Fukao and Y. Miyamoto, Phys. Rev. E **61**, 1743 (2000).
[5] K. Fukao and Y. Miyamoto, Europhys. Lett. **46**, 649 (1999).
[6] G. B. DeMaggio, W. E. Frieze, D. W. Gidley, M. Zhu, H. A. Hristov, and A. F. Yee, Phys. Rev. Lett. **78**, 1524 (1997).
[7] N. Satomi, A. Takahara, and T. Kajiyama, Macromolecules **32**, 4474 (1999).
[8] J. L. Keddie, R. A. L. Jones, and R. A. Cory, Faraday Discuss. **98**, 1 (1994).
[9] D. S. Fryer, P. F. Nealey, and J. J. de Pablo, Macromolecules **33**, 6439 (2000).
[10] D. S. Fryer, P. F. Nealey, and J. J. de Pablo, J. Vac. Sci. Technol. B **18**, 3376 (2000).
[11] W. E. Wallace, J. H. van Zanten, and W.-l. Wu, Phys. Rev. E **52**, R3329 (1995).
[12] B. Frank, A. P. Gast, T. P. Russell, H. U. Brown, and C. Hawker, Macromolecules **29**, 6531 (1996).
[13] X. Zheng, M. H. Rafailovich, J. Sokolov, Y. Strzhemechny, S. A. Schwarz, B. B. Sauer, and M. Rubinstein, Phys. Rev. Lett. **79**, 241 (1997).
[14] L. Xie, G. B. DeMaggio, W. E. Freize, J. DeVries, D. W. Gidley, H. A. Hristov, and A. F. Yee, Phys. Rev. Lett. **74**, 4947 (1995).
[15] O. Kahle, U. Wielsch, H. Metzner, J. Bauer, C. Uhlig, and C. Zawatzki, Thin Solid Films **313**, 803 (1988).
[16] G. Reiter, Europhys. Lett. **23**, 579 (1993).
[17] G. Reiter, Macromolecules **27**, 3046 (1994).
[18] J. Colmenero and A. Arbe, Phys. Rev. B **57**, 13 508 (1998).
[19] B. Frick and D. Richter, Science **267**, 1939 (1995).
[20] C. A. Angell, Science **267**, 1924 (1995).
[21] Certain commercial equipment and materials are identified in this paper in order to specify adequately the experimental procedure. In no case does such identification imply recommendation by the National Institute of Standards and Technology nor does it imply the material or equipment identified is necessarily the best available for this purpose.
[22] J. F. Anker and C. J. Majkrzak, Proc. SPIE **1738**, 260 (1992).
[23] P. M. Gehring and D. A. Neumann, Physica B **241–243**, 64 (1998).
[24] C. L. Soles, E. K. Lin, J. F. Douglas, and W.-l. Wu, Phys. Rev. E (submitted).
[25] U. Buchenau and R. Zorn, Europhys. Lett. **18**, 523 (1992).
[26] S. Granick, Science **253**, 1374 (1991).